

# Photophysics and Photochemistry of Nitroanthracenes

## Part 1.—Primary Processes in the Photochemical Reactions of 9-Benzoyl-10-nitroanthracene and 9-Cyano-10-nitroanthracene studied by Steady-state Photolysis and Nanosecond Laser Photolysis

Kumao Hamanoue,\* Toshihiro Nakayama, Kiminori Ushida, Kanji Kajiwara and Shigenobu Yamanaka

Department of Chemistry, Kyoto Institute of Technology, Matsugasaki, Sakyo-ku, Kyoto 606, Japan

The genuine phosphorescence spectra of the title compounds (XNA) have been clearly observed at 77 K in EPA (diethyl ether–isopentane–ethanol 5 : 5 : 2 volume ratio). Also, the time-resolved absorption spectra obtained at the end of nanosecond laser pulse at 77 K (in EPA) and at room temperature (in ethanol and benzene) have been ascribed to the superposition of the absorptions of the lowest triplet XNA [ $^3\text{XNA}(T_1)$ ] on those of the corresponding anthryloxy radicals (XAO $\cdot$ ). The decay of  $^3\text{XNA}(T_1)$  is not accompanied by the formation of XAO $\cdot$  and the following results are obtained. (1) In ethanol at room temperature, the first-order decay of XAO $\cdot$  corresponds to hydrogen-atom abstraction by XAO $\cdot$  from the solvent, giving rise to the formation of corresponding anthrols (XAOH), while the second-order reaction of XAO $\cdot$  with nitrogen(II) oxide (NO $\cdot$ ) yields the corresponding nitrosoanthrones (XNSAN) which decompose very slowly into XAO $\cdot$  and NO $\cdot$  followed by the rapid formation of XAOH. (2) In benzene at room temperature no formation of XAOH is observed, but there exists an equilibrium between XAO $\cdot$ (+NO $\cdot$ ) and XNSAN. All these results support our previous conclusion that the nitro  $\rightarrow$  nitrite rearrangement of XNA does not occur for the lowest triplet states of  $\pi\pi^*$  character but does occur for the higher triplet states of  $n\pi^*$  character, followed by the cleavage of the nitrites to XAO $\cdot$  and NO $\cdot$ .

In previous papers,<sup>1–4</sup> we have reported that steady-state photolysis of 9-benzoyl-10-nitroanthracene (BNA) and 9-cyano-10-nitroanthracene (CNA) gives rise to the formation of corresponding anthryloxy radicals (XAO $\cdot$ ), anthrols (XAOH) or their anions under appropriate conditions, and that the form of the final products is dependent on the basicity, polarity and rigidity of the medium as well as the temperature. Moreover, picosecond and nanosecond laser photolyses of these nitroanthracenes (XNA) have revealed that intersystem crossing from the lowest excited singlet  $\pi\pi^*$  [ $S_1(\pi\pi^*)$ ] states to the higher triplet  $n\pi^*$  [ $T_n(n\pi^*)$ ] states, located near to or very slightly below the  $S_1$  ( $\pi\pi^*$ ) states, is very rapid with rate constants  $>10^{11} \text{ s}^{-1}$ ,<sup>5</sup> and the absorption spectra of the lowest triplet  $\pi\pi^*$  [ $T_1(\pi\pi^*)$ ] states and XAO $\cdot$  grow in simultaneously.<sup>2</sup> We have therefore concluded that the nitro  $\rightarrow$  nitrite rearrangement of XNA does not occur for the  $T_1(\pi\pi^*)$  states but does occur for the  $T_n(n\pi^*)$  states, followed by the cleavage of the nitrites to XAO $\cdot$  and nitrogen(II) oxide (NO $\cdot$ ).

Time-resolved absorption spectra for the nanosecond–microsecond time regime have been recorded by the separate measurements of absorptions at a number of desired wavelengths, each following a single laser shot, *i.e.* point-to-point measurements. The probing-light intensity transmitted by the sample is detected by a photomultiplier and the trace of the resulting electrical waveform on the screen of an oscilloscope is recorded photographically. A hand-drawn plot of the calculated absorbance at a given wavelength is then performed and these operations have to be repeated at each monochromator setting. Since some inaccuracy and arbitrariness are unavoidable for the absorption spectra recorded by such a conventional method, and since the time-resolved absorption spectra ascribed to the superposition due to the absorptions of the  $T_1$  states of XNA on those of XAO $\cdot$  are very weak and are not well resolved, the point-to-point measurements are not good enough for the detailed spectroscopic discussion.

To overcome these difficulties, we have recently constructed a convenient nanosecond laser photolysis system equipped with a multichannel detector controlled by a per-

sonal computer.<sup>6</sup> By this photolysis system, the well resolved transient absorption spectra and the decay profiles of transient absorptions (and emissions) for the nanosecond–millisecond time regime have been recorded easily. This paper deals with a re-investigation of the primary process in the photochemical reaction of XNA, because Testa and Wild disputed our previous results based on a small quantum yield for the photoreduction of 9-nitroanthracene in poly(vinyl butyral) film<sup>7</sup> and no observation of the intrinsic phosphorescence from 9-nitroanthracene.<sup>8</sup>

### Experimental

The details of the methods of preparation and purification of XNA have been given previously.<sup>1</sup> GR-grade isopentane (Wako) was further purified by passing it through an alumina column. Uvasol diethyl ether (Merck) and all the other solvents (Wako, GR grade) were used without further purification. Unless stated otherwise, the sample solutions in a cell of 1 cm pathlength were degassed by several freeze–pump–thaw cycles, and steady-state photolysis was carried out using an USH-500D super-high-pressure mercury lamp; light of 366 nm monochromatic wavelength was selected by a combination of two Toshiba UV-35 and UV-D35 glass filters with a filter solution ( $\text{CuSO}_4 \cdot 5\text{H}_2\text{O}$ ,  $100 \text{ g dm}^{-3}$ , pathlength 3 cm).

The absorption spectra were recorded using a Hitachi 200-20 spectrophotometer, and the phosphorescence and their excitation spectra were recorded using a Hitachi MPF-4 spectrophosphorimeter with a Hamamatsu R928 photomultiplier whose spectral response extended up to 900 nm. Nanosecond laser photolysis was performed using the second harmonic (347.2 nm, pulse width = 20 ns) from a home-made Q-switched ruby laser.<sup>6</sup> A pulsed xenon flash lamp (Unisoku USP543S) was used as a probing-light source and the time-resolved absorption spectra over a wavelength range of 200 nm were recorded using a multichannel analyser composed of a polychromator (Unisoku M200), an image intensifier

(Hamamatsu V3347U) and a linear position-sensitive detector (Unisoku USP501) controlled by a personal computer (NEC PC-9801RA). Operating the image intensifier in gated or continuous mode, the time-resolved absorption spectra for the nanosecond–millisecond time regime could be recorded very easily from one excitation laser shot. The decays of transient absorptions and phosphorescences were analysed by means of a combination of a photomultiplier (Hamamatsu R666 or RCA 8575) with a storage oscilloscope (Iwatsu TS-8123) controlled by the personal computer.

### Results and Discussion

The changes of absorption spectra upon steady-state photolysis of XNA in ethanol at room temperature are shown in Fig. 1. We have already identified the photoproducts as 10-benzoyl-9-anthrol for BNA and 10-cyano-9-anthrol (and a small amount of 9-cyano-10-anthryloxy anion) for CNA.<sup>2</sup> The broad absorption spectra (at 330–500 nm) due to the photoproducts increased slightly up to 1 h after the end of steady-state photolysis.<sup>9</sup> As will be discussed later, we ascribed this absorption increment to the decomposition of nitrosoanthrones (XNSA, *i.e.* the 9-benzoyl and 9-cyano compounds) into XAO\* and NO\* followed by the rapid formation of XAOH. Addition of ferrocene caused no change in the decrease of XNA during photolysis, while the dissolved oxygen enhanced the decrease of XNA (see the inserts to the figures). This effect of oxygen may be due to the decrease in the yield of XAOH that has absorption in a similar wavelength range to that of XNA. As shown in Fig. 2, the photochemical reaction of XNA in EPA (diethyl ether–isopentane–ethanol 5 : 5 : 2 volume ratio) at 77 K was different from that in ethanol at room temperature. We have already confirmed the photoproduct in EPA at 77 K to be XAO\*.<sup>2</sup> Formation of XAO\* was also observed in benzene at room temperature, as shown in the inserts to the figures,

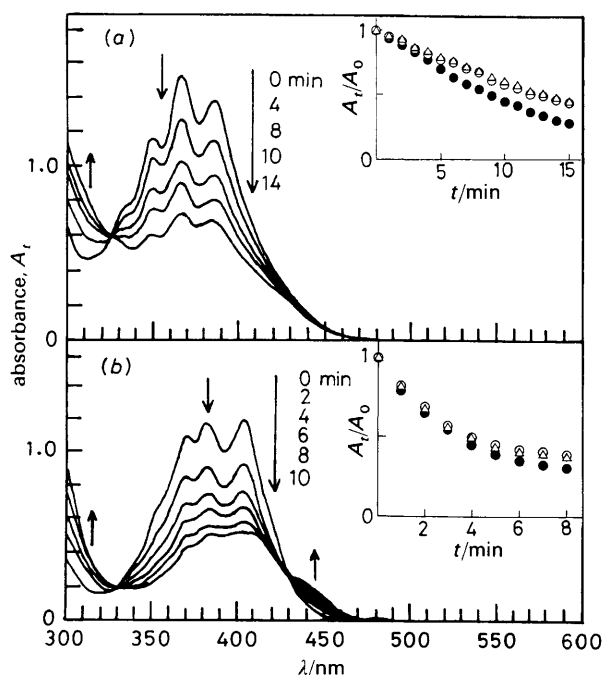


**Fig. 1** Changes of absorption spectra upon steady-state photolysis of BNA (a) and CNA (b) in ethanol at room temperature. Inserts are the relative absorption decreases of XNA measured in the absence (O) and presence of oxygen (●,  $ca. 3 \times 10^{-3} \text{ mol dm}^{-3}$ ) and ferrocene (Δ,  $5 \times 10^{-4} \text{ mol dm}^{-3}$ ), (a) at 368 nm, (b) at 385 nm

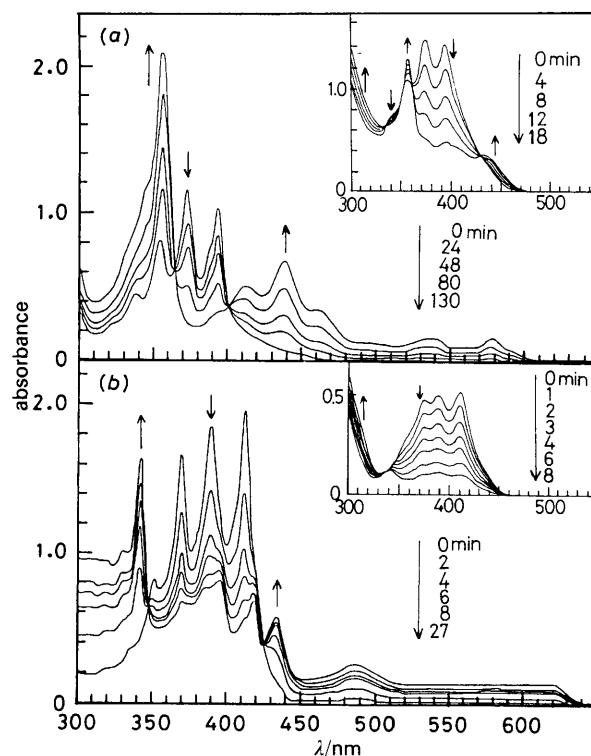
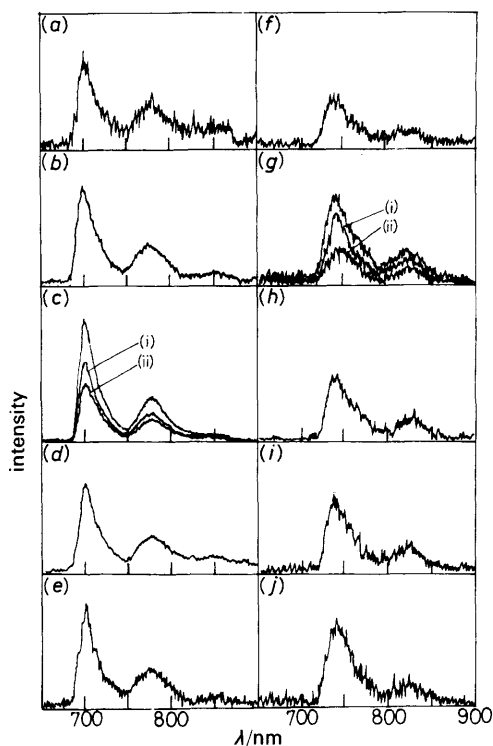


**Fig. 2** Changes of absorption spectra upon steady-state photolysis of BNA (a) and CNA (b) in EPA at 77 K. Inserts are the results in benzene at room temperature

although the absorption band of 9-cyano-10-anthryloxy radical was very weak.

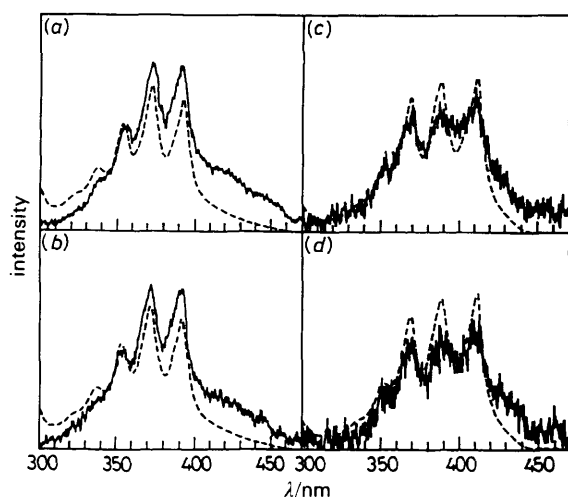
The emission spectra of XNA shown in Fig. 3 were recorded in EPA at 77 K, indicating that the excitation wavelength did not affect the spectral profile; no emissions were observed in the wavelength range  $< 650 \text{ nm}$ . The emission excitation spectra (Fig. 4, full lines) were not affected by the monitoring wavelength, and the spectra obtained were identical with the absorption spectra (broken lines) of XNA. In connection with the emission spectra reported by us for 9-nitroanthracene<sup>10</sup> and BNA,<sup>2</sup> Testa<sup>8</sup> suggested that these spectra should be recorded at longer excitation wavelengths, *i.e.* 458–466 nm. To do so the spectral measurements should be performed at much higher sample concentrations; however, the spectra recorded with 440–460 nm excitation were identical with those in Fig. 3. Testa<sup>8</sup> also suggested that the spectra observed by us were due to the emission of anthracene derivatives generated by secondary photochemistry. If this were correct, the emission intensity should increase with increasing photolysis time. In contrast, as indicated by (i) and (ii) in Fig. 3(c) and (g), the emission intensity observed after steady-state photolysis in EPA at 77 K decreased with increasing photolysis time, but no change in the spectral profile was observed. This decrease in the emission intensity upon photolysis is consistent with the fact that XNA undergoes photochemical reaction even in a frozen matrix at 77 K, leading to the formation of XAO\* [*cf.* Fig. 2(a) and (b)]. A similar result has also been obtained for 9-nitroanthracene.<sup>10</sup> Thus, one can safely conclude that the emission spectra observed by us do not originate from the photoproducts but are due to genuine phosphorescence from XNA.

Fig. 5 shows the time-resolved absorption spectra of XNA, recorded for the high- and low-concentration samples in EPA at 77 K. For the high-concentration samples [(a) and (c)], no transient absorptions were recorded in the wavelength range  $< 400 \text{ nm}$  owing to the intensity loss of probing light caused



**Fig. 3** Phosphorescence spectra of XNA in EPA at 77 K recorded at various excitation wavelengths with band-pass of 6 nm for BNA and 15 nm for CNA. (a)–(e) BNA at 330, 354, 372, 390 and 415 nm; (f)–(j) CNA at 330, 370, 390, 410 and 430 nm. In (c) and (g), the spectra shown by (i) and (ii) were recorded after steady-state photolysis in EPA at 77 K: (c) (i) 10, (ii) 20 min; (g) (i) 2, (ii) 4 min

by the sample absorption; however, the spectra with bands A and B<sub>2</sub> were identical with those recorded by a photographic method.<sup>2,5</sup> For the low-concentration samples [(b), (d)], the time-resolved absorption spectra had additional absorptions (bands B<sub>1</sub>), and bands B<sub>1</sub> and B<sub>2</sub> were characteristic of the absorption spectra due to XAO\* produced upon steady-state photolysis in EPA at 77 K [cf. Fig. 2(a) and (b)]. Although bands B<sub>1</sub> did not decay with time, bands A decayed following a single exponential function [cf. Fig. 6(a) and (b)] and the



**Fig. 4** Phosphorescence excitation spectra (—) of XNA in EPA at 77 K recorded at various monitoring wavelengths with band-pass of 6 nm. (---) Absorption spectra of XNA in EPA at 77 K recorded at 4 nm resolution. (a) BNA at 700 nm, (b) BNA at 775 nm, (c) CNA at 740 nm, (d) CNA at 825 nm

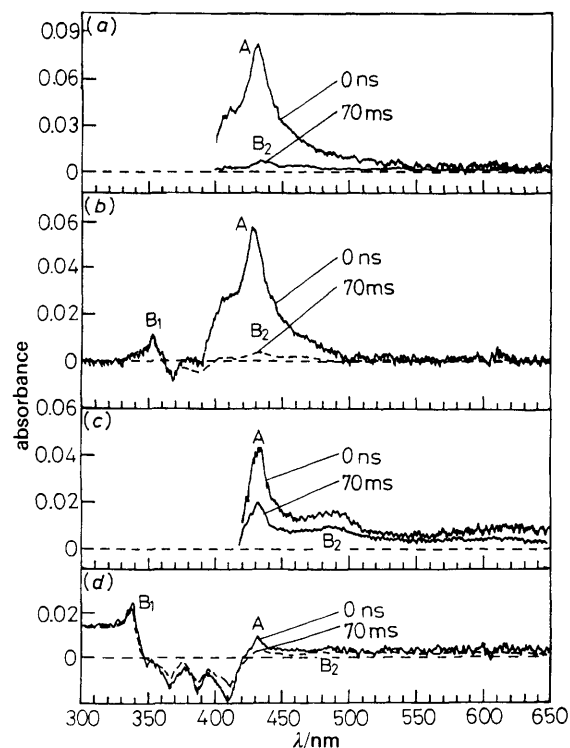


**Fig. 5** Time-resolved absorption spectra obtained by nanosecond laser photolysis of XNA in EPA at 77 K. (a) BNA ( $4.8 \times 10^{-4}$  mol  $\text{dm}^{-3}$ ), (b) BNA ( $7.2 \times 10^{-5}$  mol  $\text{dm}^{-3}$ ), (c) CNA ( $2.9 \times 10^{-4}$  mol  $\text{dm}^{-3}$ ), (d) CNA ( $8.1 \times 10^{-5}$  mol  $\text{dm}^{-3}$ )

lifetimes were equal to the phosphorescence lifetimes [cf. Fig. 6(c) and (d)]. Thus, the decay components in bands A can be safely assigned to the triplet-triplet ( $T' \leftarrow T_1$ ) absorptions of XNA, originating from  $T_1$  states of  $\pi\pi^*$  character. In fact, bands A are very similar to the  $T' \leftarrow T_1$  absorption spectra of several anthracenes such as 9-acetylanthracene,<sup>11,12</sup> 9-cyanoanthracene,<sup>13,14</sup> and 9- and 9,10-dibromoanthracene.<sup>15</sup> Of course, a small amount of absorption (bands B<sub>2</sub>) due to XAO\* is contained in bands A as the non-decay components.

Except for the decrease in intensity of bands B<sub>1</sub> with time, the time-resolved absorption spectra in ethanol at room temperature shown in Fig. 7 were essentially identical with those

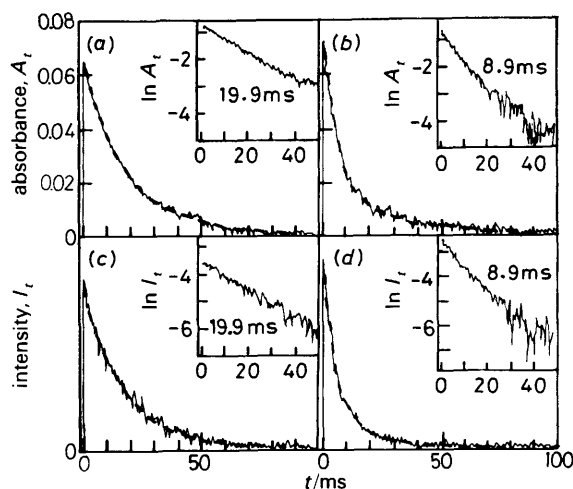


**Fig. 6** Single-exponential decays of  $T' \leftarrow T_1$  absorptions [(a), (b)] and phosphorescence [(c), (d)] of XNA in EPA at 77 K. (---) Simulated curves with inserted decay constants. (a) BNA at 430 nm, (b) CNA at 430 nm, (c) BNA at 700 nm, (d) CNA at 740 nm

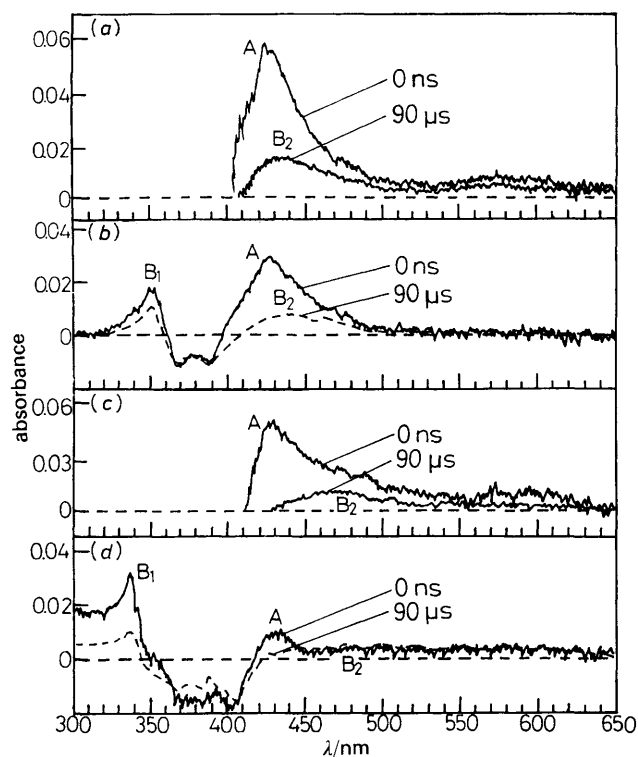


**Fig. 7** Time-resolved absorption spectra obtained by nanosecond laser photolysis of XNA in ethanol at room temperature. (a) BNA ( $4.3 \times 10^{-4} \text{ mol dm}^{-3}$ ), (b) BNA ( $6.5 \times 10^{-5} \text{ mol dm}^{-3}$ ), (c) CNA ( $1.8 \times 10^{-3} \text{ mol dm}^{-3}$ ), (d) CNA ( $3.8 \times 10^{-4} \text{ mol dm}^{-3}$ )

in EPA at 77 K. This is reasonable, because steady-state photolysis in EPA at 77 K gave rise to the formation of XAO\* as the stable products, while XAOH was produced in ethanol at room temperature, indicating that the absorption of XAO\* in ethanol at room temperature should decay with time. In fact, as shown in Fig. 8, the intensity of bands A monitored at 430 nm decayed initially following a single-exponential function [(a), (b)] and then decayed slowly toward zero-absorptions [(c), (d)]. Clearly, the rapid decay components with rate con-

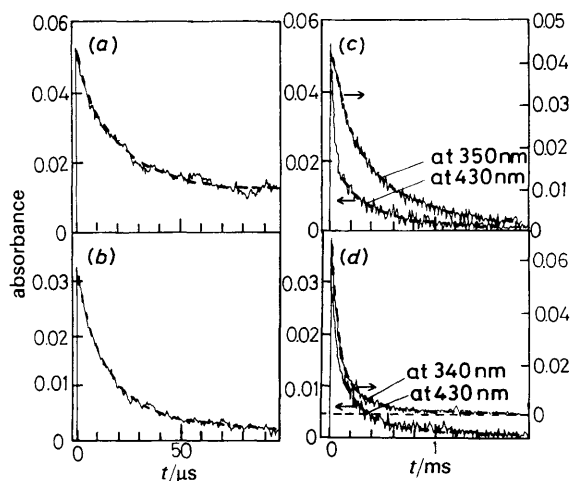


**Fig. 8** Single-exponential decays of the  $T' \leftarrow T_1$  absorptions of XNA [(a), (b)] and double-component decays of XAO\* [(c), (d)] in ethanol at room temperature. (---) Simulated curves with decay constants; (a) BNA at 430 nm,  $k_T = 7.40 \times 10^4 \text{ s}^{-1}$ ; (b) CNA at 430 nm,  $k_T = 9.71 \times 10^4 \text{ s}^{-1}$ ; (c) BNA,  $k_1 = 1 \times 10^3 \text{ s}^{-1}$ ,  $k_2 = 1 \times 10^9 \text{ dm}^3 \text{ mol}^{-1} \text{ s}^{-1}$ ; (d) CNA,  $k_1 = 2 \times 10^3 \text{ s}^{-1}$ ,  $k_2 = 1 \times 10^9 \text{ dm}^3 \text{ mol}^{-1} \text{ s}^{-1}$

stant  $k_T$  are the  $T' \leftarrow T_1$  absorptions of XNA, and the slow decay components are the absorptions of XAO\*.

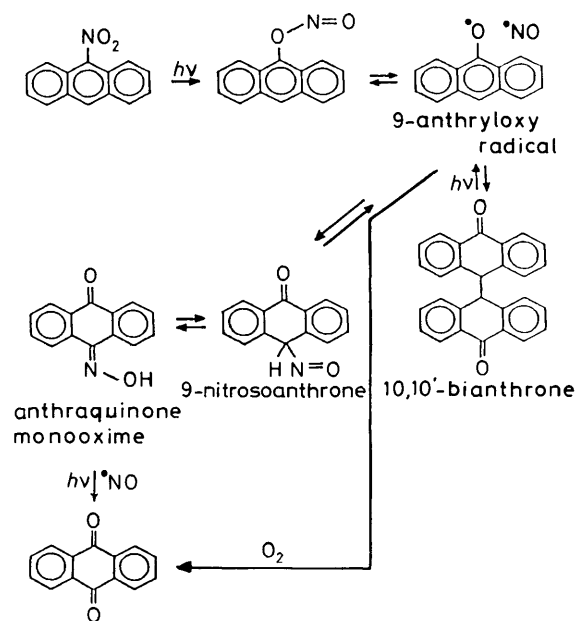
For the photochemical reaction of 9-nitroanthracene in acetone at room temperature, Chapman *et al.*<sup>16</sup> proposed Scheme 1. Although they could not identify 9-anthryloxy radical, we confirmed the existence of this radical as an intermediate in the photochemistry of 9-nitroanthracene.<sup>10,17</sup> We thus believe that XAO\* abstracts a hydrogen atom from ethanol following first-order reaction kinetics and XAOH is produced. Since no formation of 10,10'-bianthrone derivatives was detected by GC-MS analysis and since addition of NO\* accelerated the decay of XAO\*,<sup>9</sup> the second-order recombination of XAO\* with NO\* may produce XNSAN. Although Chapman *et al.* proposed the formation of anthraquinone monoxime *via* 9-nitrosoanthracene (*cf.* Scheme 1), the formation of such anthraquinone monoximes *via* XNSAN is improbable owing to the lack of hydrogen atoms in the *meso*-position of XNA. If such a reaction does occur, one cannot explain the existence of XAO\* as the stable product in benzene at room temperature.

Based on the above discussion, the most probable curve fitting for the slow decays of bands A (monitored at 430 nm) and bands B<sub>1</sub> (monitored at 350 nm for BNA and 340 nm for CNA) can be achieved by a combination of first- and second-order reaction kinetics with rate constants  $k_1$  and  $k_2$ , respectively. The theoretical decay function is then expressed as the solution of the following two differential equations,

$$-\frac{d[\text{XAO}^*]_t}{dt} = (k_1 + k_2[\text{NO}^*]_t)[\text{XAO}^*]_t \quad (1)$$

$$-\frac{d[\text{NO}^*]_t}{dt} = k_2[\text{NO}^*]_t[\text{XAO}^*]_t \quad (2)$$

where  $[\text{XAO}^*]_t$  and  $[\text{NO}^*]_t$  are the concentrations of XAO\* and NO\* at time  $t$ . Assuming the initial concentration of XAO\* to be equal to that of NO\*, and estimating the molar absorption coefficients of 9-benzoyl-10-anthryloxy radical ( $17000$  and  $7000 \text{ dm}^3 \text{ mol}^{-1} \text{ cm}^{-1}$  at 350 and 430 nm) and 9-cyano-10-anthryloxy radical ( $13000$  and  $5500 \text{ dm}^3 \text{ mol}^{-1} \text{ cm}^{-1}$  at 340 and 430 nm) from the absorption spectra shown in Fig. 2(a) and (b), the values of  $k_1$  and  $k_2$  can be determined by the best fit of theoretical decay curves to experimental



**Scheme 1**

curves. The numerical integration of eqn. (1) and (2) is performed by the Runge-Kutta method, changing the values of  $k_1$  and  $k_2$  as the fitting parameters; since the experimental decay curves in Fig. 8(c) and (d) can also be reproduced by the non-linear least-squares method as a sum of following two exponential terms,

$$[\text{XAO}^*]_t = C_1 \exp(-at) + C_2 \exp(-bt) \quad (3)$$

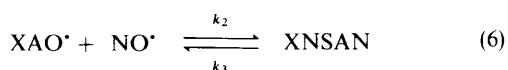
the choice of parameters of  $k_1$  ( $0 \leq k_1 < a$ ) and  $k_2$  is made from the solution of the equations

$$\ln \left[ \frac{1}{a - k_1} \left( \frac{C_1 a + C_2 b}{C_1 + C_2} - k_1 \right) \right] + \frac{1}{[\text{XAO}^*]_0} \times \left( \frac{C_1}{a} + \frac{C_2}{b} \right) \left( k_1 - \frac{C_1 a + C_2 b}{C_1 + C_2} \right) = 0 \quad (4)$$

$$k_2 = \frac{1}{[\text{XAO}^*]_0} \left( \frac{C_1 a + C_2 b}{C_1 + C_2} - k_1 \right) \quad (5)$$

where  $[\text{XAO}^*]_0$  is the concentration of  $\text{XAO}^*$  at time zero. The best-fit curves shown by broken curves in Fig. 8(c) and (d) can reproduce the decays of  $\text{XAO}^*$  and the values of  $k_2$  obtained are of the order of that for a diffusion-controlled reaction. Thus, the formation of  $\text{XNSAN}$  by the second-order reaction of  $\text{XAO}^*$  with  $\text{NO}^*$  is reasonable. Since the absorptions of  $\text{XAOH}$  increased slowly up to 1 h after steady-state photolysis, as stated previously, we further propose that  $\text{XNSAN}$  produced in ethanol at room temperature decomposes very slowly into  $\text{XAO}^*$  and  $\text{NO}^*$  followed by the rapid formation of  $\text{XAOH}$ .

The time-resolved absorption spectra obtained in benzene at room temperature were essentially identical with those obtained in ethanol, as shown in Fig. 9. However, the intensity ratios of bands  $B_1$  at 90  $\mu\text{s}$  delay to those at 0 ns delay in benzene were greater than those in ethanol. In accordance with this, we confirmed that the intensities of bands  $B_1$  in benzene (monitored at 350 nm for BNA and 340 nm for CNA) decayed more slowly than those in ethanol. Although the intensities of bands A in benzene (monitored at 430 nm) decayed rapidly with rate constant  $k_T$  [Fig. 10(a) and (b)], the residual absorptions due to  $\text{XAO}^*$  decayed very slowly. In order to obtain details of these slow decay components, we recorded the decay curves over a much longer timescale as shown in Fig. 10(c) and (d). Clearly, bands A (monitored at 430 nm) and bands  $B_1$  (monitored at 350 nm for BNA and 340 nm for CNA) decayed toward constant absorptions, but no change in the spectral profile was observed after the end of absorption decay [cf. Fig. 9(c) and (f)]. These results are reasonable, because  $\text{XAOH}$  is not produced upon steady-state photolysis in benzene at room temperature, but  $\text{XAO}^*$  is produced as the stable photoproducts indicating that the hydrogen-atom abstraction by  $\text{XAO}^*$  from benzene is impossible. Since addition of  $\text{NO}^*$  also accelerated the decay of  $\text{XAO}^*$  in benzene,<sup>9</sup> and since steady-state photolysis of  $\text{XNA}$  in benzene revealed the formation of  $\text{XAO}^*$  as the stable product, we propose that the decomposition of  $\text{XNSAN}$  into  $\text{XAO}^*$  and  $\text{NO}^*$  is very rapid compared with that in ethanol, finally leading to the following equilibrium,<sup>†</sup>



<sup>†</sup> After steady-state photolysis of  $\text{XNA}$  in benzene at room temperature, the absorption spectra of  $\text{XAO}^*$  increased slightly.<sup>9</sup> This may be due to the fact that a small amount of dissolved  $\text{NO}^*$  transfers to the gas phase and the equilibrium given by eqn. (6) is shifted to the left, leading to partial decomposition of  $\text{XNSAN}$  into  $\text{XAO}^*$  and  $\text{NO}^*$ .

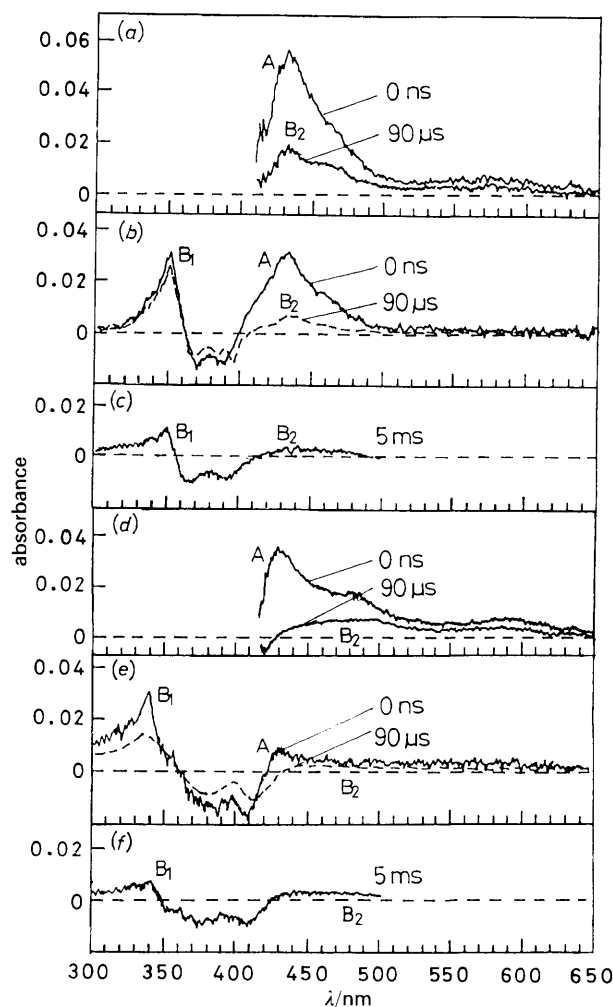


Fig. 9 Time-resolved absorption spectra obtained by nanosecond laser photolysis of  $\text{XNA}$  in benzene at room temperature. (a) BNA ( $3.8 \times 10^{-4} \text{ mol dm}^{-3}$ ), (b) BNA ( $5.7 \times 10^{-5} \text{ mol dm}^{-3}$ ), (c) BNA ( $5.7 \times 10^{-5} \text{ mol dm}^{-3}$ ), (d) CNA ( $4.6 \times 10^{-4} \text{ mol dm}^{-3}$ ), (e) CNA ( $9.2 \times 10^{-5} \text{ mol dm}^{-3}$ ), (f) CNA ( $9.2 \times 10^{-5} \text{ mol dm}^{-3}$ )

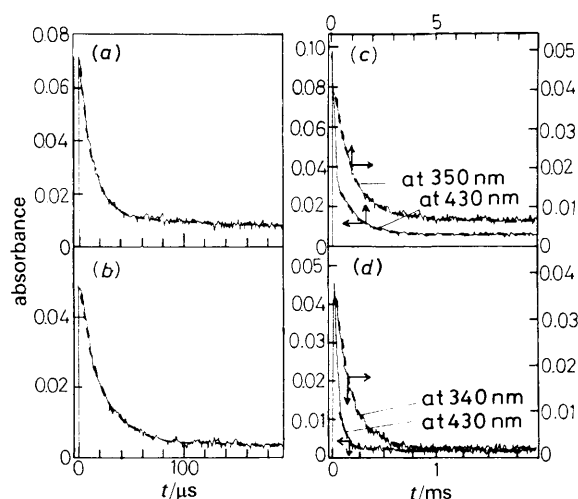


Fig. 10 Single-exponential decays of the  $T^* \leftarrow T_1$  absorptions of  $\text{XNA}$  [(a), (b)] and double-component decays of  $\text{XAO}^*$  [(c), (d)] in benzene at room temperature. (---) Simulated curves with decay constants: (a) BNA at 430 nm,  $k_T = 5.34 \times 10^4 \text{ s}^{-1}$ ; (b) CNA; (c) BNA at 430 nm,  $k_T = 6.06 \times 10^4 \text{ s}^{-1}$ ;  $k_2 = 5 \times 10^9 \text{ dm}^3 \text{ mol}^{-1} \text{ s}^{-1}$ ,  $k_3 = 5 \times 10^2 \text{ s}^{-1}$ ; (d) CNA,  $k_2 = 3 \times 10^9 \text{ dm}^3 \text{ mol}^{-1} \text{ s}^{-1}$ ,  $k_3 = 3 \times 10^3 \text{ s}^{-1}$

In this case, the concentration of XAO<sup>•</sup> should be equal to that of NO<sup>•</sup> at any delay time. Thus, the change of [XAO<sup>•</sup>]<sub>t</sub> with time is given by

$$-\frac{d\Delta[\text{XAO}^\bullet]_t}{dt} = (k_2\Delta[\text{XAO}^\bullet]_t + 2k_2[\text{XAO}^\bullet]_e + k_3)\Delta[\text{XAO}^\bullet]_t \quad (7)$$

$$\Delta[\text{XAO}^\bullet]_t = [\text{XAO}^\bullet]_t - [\text{XAO}^\bullet]_e \quad (8)$$

and the following equations can easily be derived:

$$[\text{XAO}^\bullet]_t - [\text{XAO}^\bullet]_e = \frac{2k_2[\text{XAO}^\bullet]_e + k_3}{B \exp\{(2k_2[\text{XAO}^\bullet]_e + k_3)t\} - k_2} \quad (9)$$

$$B = k_2 + \frac{2k_2[\text{XAO}^\bullet]_e + k_3}{[\text{XAO}^\bullet]_0 - [\text{XAO}^\bullet]_e} \quad (10)$$

where [XAO<sup>•</sup>]<sub>e</sub> is the equilibrium concentration of XAO<sup>•</sup> and k<sub>3</sub> is the first-order rate constant for decomposition of XNSAN into XAO<sup>•</sup> and NO<sup>•</sup>. Thus, the values of k<sub>2</sub> and k<sub>3</sub> can be determined by the best fit of theoretical decay curves to experimental curves. In Table 1, we list the values of rate constants obtained so far in ethanol and benzene at room temperature. The values of k<sub>1</sub>, k<sub>2</sub> and k<sub>3</sub> determined from the decays of bands A were identical to those determined from the decays of bands B<sub>1</sub>.

In aerated solvents at room temperature, the single-exponential decays of T' ← T<sub>1</sub> absorptions were faster than those in deaerated solvents (cf. Table 2) and no long-lived (nor residual) absorptions, as observed in deaerated solvents, were observed. This indicates that oxygen quenches not only the T<sub>1</sub> states of XNA [<sup>3</sup>XNA(T<sub>1</sub>)] but also XAO<sup>•</sup>. The quenching of XAO<sup>•</sup> by oxygen is consistent with the fact that the decrease of XNA during steady-state photolysis in ethanol is enhanced upon addition of air, because the absorptions of XNA overlap with those of XAOH (cf. Fig. 1). On an assumption of oxygen concentration to be ca. 3 × 10<sup>-3</sup> mol dm<sup>-3</sup>, the values of triplet quenching rate constants (k<sub>q</sub>) by oxygen were calculated as listed in Table 2. In the presence of ferrocene (5 × 10<sup>-4</sup> mol dm<sup>-3</sup>), only the T' ← T<sub>1</sub> absorptions of XNA were quenched; the values of k<sub>T</sub> in the presence of ferrocene were greater than those in the absence of ferrocene, while those of k<sub>1</sub> and k<sub>2</sub> were not affected upon addition of ferrocene (cf. Tables 1 and 2). This lack of effect of ferrocene

on the decay of XAO<sup>•</sup> is consistent with the fact that addition of ferrocene does not affect the decrease of XNA during steady-state photolysis in ethanol (cf. inserts in Fig. 1).

### Conclusion

All the results obtained so far indicate that the time-resolved absorption spectra at 0 ns delay shown in Fig. 5, 7 and 9 are a superposition due to the absorptions of <sup>3</sup>XNA(T<sub>1</sub>) on those of XAO<sup>•</sup>. Similar time-resolved absorption spectra have also been obtained by picosecond laser photolysis at room temperature,<sup>2,5</sup> where the rise times of transient absorptions are ca. 70 ps and no measurable change in the spectral profile is observed in the picosecond time regime. In the previous paper,<sup>5</sup> we ascribed the lack of fluorescence in nitroanthracenes to the efficient intersystem crossing (ISC) from the S<sub>1</sub>(ππ\*) state to the T<sub>n</sub>(nπ\*) state which is located near to or very slightly below the S<sub>1</sub>(ππ\*) state, because El-Sayed's selection rule predicts that ISC between two states with different types of electronic character (e.g. nπ\* ↔ ππ\*) should be at least an order of magnitude greater than ISC between two states with the same type of electronic character (e.g. nπ\* ↔ nπ\* or ππ\* ↔ ππ\*).<sup>18</sup> The S<sub>1</sub>(ππ\*) → T<sub>n</sub>(nπ\*) ISC rate may be very rapid because of favourable spin-orbit coupling and a large Franck-Condon factor; on the other hand, the direct S<sub>1</sub>(ππ\*) → T<sub>1</sub>(ππ\*) ISC will be insignificant because of the weak spin-orbit coupling and the extremely small Franck-Condon factor. Since the large S<sub>1</sub>(ππ\*)-T<sub>1</sub>(ππ\*) splitting makes it likely that there exists a second or third triplet state near the S<sub>1</sub>(ππ\*) state, the indirect path [S<sub>1</sub>(ππ\*) → T<sub>n</sub>(nπ\*) → T<sub>1</sub>(ππ\*)] is important for the photochemistry of nitroanthracenes. Based on the suggestion of Chapman *et al.*<sup>16</sup> that the nitro → nitrite rearrangement of 9-nitroanthracene occurs for an nπ\* excited state (cf. Scheme 1), we conclude that <sup>3</sup>XNA(T<sub>1</sub>) and XAO<sup>•</sup> are produced simultaneously *via* the higher T<sub>n</sub>(nπ\*) states, because the S<sub>1</sub> states of XNA are clearly of ππ\* character and the participation of the S<sub>1</sub> states in the photochemistry has been ruled out.<sup>2,5</sup> In summary, we propose the following scheme for the photochemical reaction of XNA in ethanol at room temperature (Scheme 2). Since no hydrogen-atom abstraction by XAO<sup>•</sup> from benzene is possible, the stable existence of XAO<sup>•</sup> in benzene is due to the equilibrium given by eqn. (6).

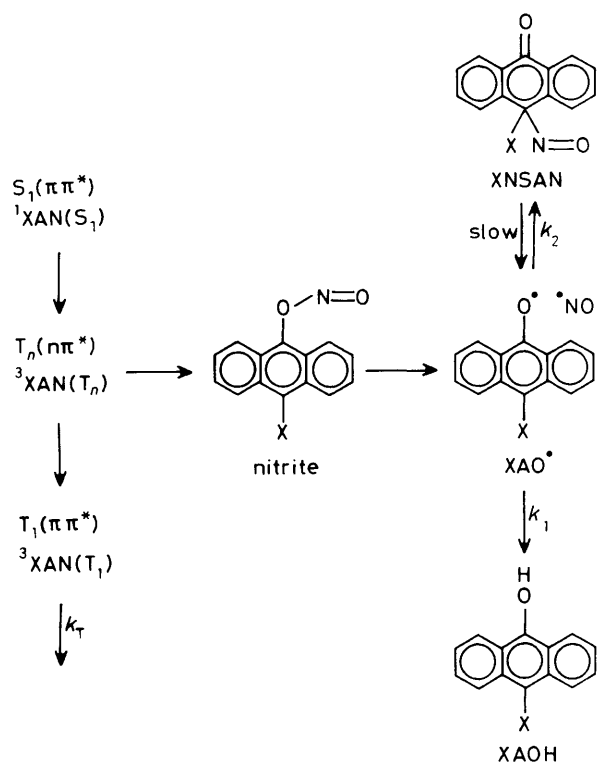
The conclusion that XAO<sup>•</sup> are not produced *via* the T<sub>1</sub>(ππ\*) states of XNA is strongly supported by the following

**Table 1** Decay constants (k<sub>T</sub>) of <sup>3</sup>XNA(T<sub>1</sub>) and those (k<sub>1</sub>, k<sub>2</sub>, k<sub>3</sub>) of XAO<sup>•</sup> at room temperature

	k <sub>T</sub> /s <sup>-1</sup>		k <sub>1</sub> /s <sup>-1</sup>	k <sub>2</sub> /dm <sup>3</sup> mol <sup>-1</sup> s <sup>-1</sup>	k <sub>2</sub> /dm <sup>3</sup> mol <sup>-1</sup> s <sup>-1</sup>	k <sub>3</sub> /s <sup>-1</sup>
	benzene	ethanol	ethanol		benzene	
BNA	5.34 × 10 <sup>4</sup>	7.40 × 10 <sup>4</sup>	ca. 1 × 10 <sup>3</sup>	ca. 1 × 10 <sup>9</sup>	ca. 5 × 10 <sup>8</sup>	ca. 5 × 10 <sup>2</sup>
CNA	6.06 × 10 <sup>4</sup>	9.71 × 10 <sup>4</sup>	ca. 2 × 10 <sup>3</sup>	ca. 1 × 10 <sup>9</sup>	ca. 3 × 10 <sup>9</sup>	ca. 3 × 10 <sup>3</sup>

**Table 2** Decay constants (k<sub>T</sub>) of <sup>3</sup>XNA(T<sub>1</sub>), their quenching rate constants (k<sub>q</sub>) and decay constants (k<sub>1</sub>, k<sub>2</sub>) of XAO<sup>•</sup> at room temperature in solutions containing oxygen (ca. 3 × 10<sup>-3</sup> mol dm<sup>-3</sup>) or ferrocene (5 × 10<sup>-4</sup> mol dm<sup>-3</sup>)

	k <sub>T</sub> /s <sup>-1</sup>		k <sub>q</sub> /dm <sup>3</sup> mol <sup>-1</sup> s <sup>-1</sup>		k <sub>1</sub> /s <sup>-1</sup>	k <sub>2</sub> /dm <sup>3</sup> mol <sup>-1</sup> s <sup>-1</sup>
	benzene	ethanol	benzene	ethanol	ethanol	
BNA (+O <sub>2</sub> )	3.13 × 10 <sup>6</sup>	4.30 × 10 <sup>6</sup>	1.03 × 10 <sup>9</sup>	1.41 × 10 <sup>9</sup>	?	?
CNA (+O <sub>2</sub> )	4.26 × 10 <sup>6</sup>	6.09 × 10 <sup>6</sup>	1.40 × 10 <sup>9</sup>	2.00 × 10 <sup>9</sup>	?	?
BNA (+ferrocene)	4.72 × 10 <sup>5</sup>	2.92 × 10 <sup>5</sup>	8.37 × 10 <sup>8</sup>	4.36 × 10 <sup>8</sup>	ca. 1 × 10 <sup>3</sup>	ca. 1 × 10 <sup>9</sup>
CNA (+ferrocene)	4.61 × 10 <sup>6</sup>	4.63 × 10 <sup>6</sup>	9.10 × 10 <sup>9</sup>	9.07 × 10 <sup>9</sup>	ca. 2 × 10 <sup>3</sup>	ca. 1 × 10 <sup>9</sup>



facts. (1) At 77 K, the  $T' \leftarrow T_1$  absorptions decay following a single-exponential function; however, there is no time-dependent intensity change in the absorption spectra of  $XAO^*$  [cf. Fig. 5(b) and (d)]. (2) Although  ${}^3XNA(T_1)$  and  $XAO^*$  decay at room temperature, the decay of  $T' \leftarrow T_1$  absorptions is not accompanied by the absorption increment of  $XAO^*$  (cf. Fig. 7 and 9). (3) In the time-resolved absorption spectra at 0 ns delay, the relative  $T_1$  yield (the intensity ratio of band A to band B<sub>1</sub>) for BNA is greater than that for CNA [cf. Fig. 5(b) and (d), Fig. 7(b) and (d) and Fig. 9(b) and (e)], while the quantum yield (0.14) for the formation of 9-benzoyl-10-anthryloxy anion at room temperature in the mixed solvent of ethanol and triethylamine is smaller than that (0.74) for the formation of 9-cyano-10-anthryloxy anion.<sup>2</sup> (4) Addition of ferrocene ( $5 \times 10^{-4}$  mol dm<sup>-3</sup>) accelerates only the decay of  $T' \leftarrow T_1$  absorptions with a quenching rate constant of the order of that for a diffusion-controlled reaction (cf. Table 2), whereas ferrocene has no effect on the decrease of XNA during steady-state photolysis (cf. inserts in Fig. 1).

From a holographic study on the photochemical reaction of 9-nitroanthracene in poly(vinyl butyral) film, Testa and Wild<sup>7</sup> obtained a small quantum yield of photoreaction, i.e.  $(8.3 \pm 1.7) \times 10^{-3}$ . Although they disputed our previous results<sup>2</sup> based on such a small quantum yield alone, we recently confirmed that the quantum yield for 9-nitroanthracene was 0.07 in ethanol,<sup>17</sup> which was ca. half of that for BNA (0.14) and one order of magnitude smaller than that for CNA (0.74).<sup>2</sup> Since 9-nitroanthracene has a hydrogen atom in the *meso*-position, the overall photochemistry of this

compound might be different from those of BNA and CNA, because the presence of hydrogen atom in the *meso*-position of 9-nitroanthracene enables 9-nitrosoanthrone to convert into anthraquinone monooxime as shown in Scheme 1. Except for the formation of anthraquinone monooxime via 9-nitrosoanthrone and the existence of a keto-enol equilibrium between anthrone and 9-anthrol, we have confirmed that the photophysics and photochemistry of 9-nitroanthracene are still identical with those of BNA and CNA.<sup>17</sup> The details of these results including objection to Testa and Wild will be published elsewhere.<sup>19</sup>

We thank Mr. Kazumitsu Sakurai for his help in the measurements of phosphorescence spectra. This work was financed by a Grant in Aid for Scientific Research from the Ministry of Education, Science and Culture of Japan (No. 62470008). K.H. also gratefully acknowledges the generous financial support of Chisso Co. Ltd.

## References

- 1 K. Hamanoue, S. Hirayama, T. Hidaka, H. Ohya, T. Nakayama and H. Teranishi, *Polym. Photochem.*, 1981, **1**, 57.
- 2 K. Hamanoue, M. Amano, M. Kimoto, Y. Kajiwara, T. Nakayama and H. Teranishi, *J. Am. Chem. Soc.*, 1984, **106**, 5993.
- 3 K. Hamanoue, S. Hirayama, M. Amano, K. Nakajima, T. Nakayama and H. Teranishi, *Bull. Chem. Soc. Jpn.*, 1982, **55**, 3104.
- 4 K. Hamanoue, K. Nakajima, M. Amano, T. Hidaka, T. Nakayama and H. Teranishi, *Polym. Photochem.*, 1983, **3**, 407.
- 5 K. Hamanoue, S. Hirayama, T. Nakayama and H. Teranishi, *J. Phys. Chem.*, 1980, **84**, 2074.
- 6 K. Ushida, T. Nakayama, T. Nakazawa, K. Hamanoue, T. Nagamura, A. Mugishima and S. Sakimukai, *Rev. Sci. Instrum.*, 1989, **60**, 617.
- 7 A. C. Testa and U. P. Wild, *J. Phys. Chem.*, 1986, **90**, 4302.
- 8 A. C. Testa, *J. Photochem. Photobiol. A*, 1989, **47**, 309.
- 9 Y. Kasiwagi, K. Okawa, K. Ushida, T. Nakayama and K. Hamanoue, Abs. Symp. Photochemistry, Kyoto, Japan, 1990, p. 123.
- 10 S. Hirayama, Y. Kajiwara, T. Nakayama, K. Hamanoue and H. Teranishi, *J. Phys. Chem.*, 1985, **89**, 1945.
- 11 K. Hamanoue, T. Hidaka, T. Nakayama and H. Teranishi, *Chem. Phys. Lett.*, 1981, **82**, 55.
- 12 K. Hamanoue, K. Nakajima, T. Hidaka, T. Nakayama and H. Teranishi, *Laser Chem.*, 1984, **4**, 287.
- 13 T. J. Kemp and J. P. Roberts, *Trans. Faraday Soc.*, 1969, **65**, 725.
- 14 E. Vander Donckt, M. R. Barthels and A. Delestinne, *J. Photochem.*, 1972/73, **1**, 429.
- 15 K. Hamanoue, S. Tai, T. Hidaka, T. Nakayama, M. Kimoto and H. Teranishi, *J. Phys. Chem.*, 1984, **88**, 4380.
- 16 O. L. Chapman, D. C. Heckert, J. W. Reasoner and S. P. Thackerberry, *J. Am. Chem. Soc.*, 1960, **88**, 5550.
- 17 Y. Yuhara, K. Ushida, T. Nakayama and K. Hamanoue, Abs. 59th Spring Meeting of the Chemical Society of Japan, Tokyo, 1990, vol. II, p. 1963.
- 18 M. A. El-Sayed, *J. Chem. Phys.*, 1963, **38**, 2834; S. K. Lower and M. A. El-Sayed, *Chem. Rev.*, 1966, **66**, 199.
- 19 K. Hamanoue, T. Nakayama, K. Ushida, K. Kajiwara and S. Yamanaka, in preparation.

Paper 1/02061G; Received 1st May, 1991